DUL 15932

8

9 10

11

31

32

33

34

35

36

37

38

TRENCH DMOS POWER TRANSISTOR WITH
FIELD-SHAPING BODY PROFILE AND
THREE-DIMENSIONAL GEOMETRY

453285

Constantin Bulucea Rebecca Rossen

FIELD OF THE INVENTION

This invention relates to power switching transistors and more particularly to vertical MOSFETs that have a gate region located in a "trench" in the semiconductor material.

BACKGROUND OF THE INVENTION

MOSFET semiconductor devices in which the gate is 12 formed in a vertically oriented groove in the semiconductor 13 material so that current flow is substantially vertical, 14 have been studied recently by several workers in the 15 field. Ueda, Takagi and Kano, in IEEE Trans. on Electron 16 Devices, Vol. ED-32 (1985) 2-6, have studied the formation 17 of vertically oriented rectangular grooves by a reactive ion 18 beam etching technique, where the structure manifests 19 reduced on-resistance and high cell packing density. Chang 20 and co-workers, in a series of papers, have also studied 21 formation of vertically oriented rectangular grooves, 22 produced by photolithographic techniques, in semiconductor 23 material and self-alignment of the groove boundaries. 24 for example, H.R. Chang, et al., IEEE Trans. on Electron 25 Devices, Vol. ED-34 (1987) 2329-2334 and references cited 26 Blanchard, in U.S. Patent No. 4,767,722, discloses 27 a method for making vertical channel DMOS structures 28 including the use of a vertically oriented rectangular 29 groove filled with doped polysilicon that serves as a gate. 30

In another research direction, Marcus, Wilson and co-workers have discussed the effects of oxidization on curved silicon surfaces of various shapes, including right angle corners and cylinders and cylindrical cavities. See, for example, Marcus and Sheng, Jour. Electrochemical Soc., Vol. 129 (1982) 1278-1282; Wilson and Marcus, Jour. Electrochemical Soc., Vol. 134 (1987). See also Yamabe and Imai, IEEE Trans. on Electron Devices, Vol. ED-34 (1987)

STP/M-799 PATENT

1 1681-1687.

Lidow and Herman, in U.S. Patents Nos. 4,593,302 and 4,680,853, disclose the fabrication of planar power MOSFETs having hexagonally shaped source cells with hexagonally shaped channels being formed beneath the source region in the semiconductor material.

6 7 8

23

24

2

3

4

5

### SUMMARY OF THE INVENTION

This invention provides an optimized version of a power 9 metal-oxide-semiconductor field-effect transistor (MOSFET) 10 that has the gate region positioned in a vertically oriented 11 12 groove or "trench" that extends from the top surface of the structure downward, using a three-dimensional cell geometry 13 14 that maximizes the gate dielectric breakdown voltage and also provides position of voltage breakdown initiation to 15 allow use of controlled bulk semiconductor breakdown. 16 breakdown is achieved by using a two-dimensional, field 17 shaping, dopant profile that includes a central deep p+ (or 18 n+) layer that is laterally adjacent to a p body layer and 19 20 that is vertically adjacent to an epitaxial layer of 21 appropriate thickness and a gate dielectric of appropriate 22 thickness in a trench.

These objects may be realized in accordance with this invention by apparatus that includes:

25 A substrate of first conductivity type, a first covering layer of first conductivity type lying on the 26 substrate, a second covering layer of second conductivity 27 28 type lying on the first covering layer and having a bottom surface, and a third covering layer of heavily doped first 29 30 conductivity type having a top surface and partly lying over the second covering layer, where a portion of the second 31 32 covering layer is heavily doped and extends vertically 33 upward through a portion of the third covering layer to the 34 top surface of the third covering layer. The apparatus also 35 includes a trench having a bottom surface and side surfaces 36 and extending downward from the top surface of the third 37 covering layer, through the third and second covering layers and through a portion of the first covering layer, where the 38

CRP/M-700 PATENT

1 bottom surface of the trench lies above a lowest part of the

- 2 bottom surface of the second covering layer. Electrically
- 3 conducting material is positioned in the trench, and an
- 4 oxide layer is positioned between this electrically
- 5 conducting material and the trench bottom and side
- 6 surfaces. Finally, three electrodes are attached to the
- 7 electrically conducting material, to the third covering
- 8 layer, and to the substrate, respectively. This apparatus
- 9 allows the transistor to avoid initiation of avalanche
- 10 breakdown adjacent to the trench.

11 12

13

14

15

16 17

18

19

20

21

22

23

24

25

26 27

28

29

30

31 32

33

34

35

38

# BRIEF DESCRIPTION OF THE DRAWINGS

Figure 1 is a schematic cross-sectional view of a trench DMOS power transistor cell in the prior art.

Figure 2A is a schematic illustration of a trench DMOS power transistor, constructed in an open-cell or stripe geometry.

Figure 28 is a schematic illustration of a trench DMOS power transistor, constructed in a closed-cell geometry.

Figures 3A and 3B are graphic illustrations of the current versus applied voltage characteristics of a representative open-cell trench DMOS transistor that has distant and closely spaced body contacts, respectively.

Figure 1 is a schematic cross-sectional view of the electrical field structure in a trench DMOS transistor that has no deep body profile, indicating the site of initial voltage breakdown.

Figure 5 is a graphic illustration of the results of a computer simulation of the electrical field lines in a trench DMOS transistor where the deep body junction is shallower than is the trench depth, indicating the site of initial voltage breakdown.

Figure 6 is a schematic cross-sectional view of a planar DMOS transistor, indicating the depletion region at the point of breakdown initiation.

Figure 7 is a schematic plan view of the oxide covering profile for trench walls with square corners.

Figure 8 is a schematic cross-sectional view of one



embodiment of the invention.

Figure 9 is a graphic illustration of the results of a computer simulation of the electrical field lines in a trenched DMOS transistor where the deep body junction lies at a greater depth than does the bottom of the trench.

Figures 10% and 10B compare the areas of intersection of intersecting trench legs, for a square-cell design and a hexagonal-cell design.

Figures 11 and 12 are graphical views of the doping concentrations at various depths below the top surface of the transistor cell shown in Figure 8, in the channel region indicated by the line CC and in a deep body region indicated by the line DD, respectively.

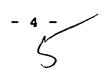
Figures 13, 14, and 15 are schematic cross-sectional views illustrating a transistor cell avalanche breakdown adjacent to the trench (Figures 13 and 14) and in the bulk material (Figures 15), showing the gate oxide thickness and the depths of the trench and epitaxial layer for three choices of pregion depth ("junction depth").

Figures 16 and 17 are schematic cross-sectional views illustrating transistor cell avalanche breakdown adjacent to the trench for decreases in epitaxial layer thickness, with all other variables unchanged.

Figures 18, 19 and 20 are schematic cross-sectional views illustrating transistor cell avalanche breakdown adjacent to the trench (Figures 18 and 19) and in the bulk of the material (Figure 20), for increasing gate oxide thickness.

Figure 21 is a schematic plan view of a group of transistor cells (square-cell geometry, for illustrative convenience), indicating the positions  $X_1X_2$  and  $X_1X_2$  of two planes for which cross-sectional views are provided in Figures 22A through 31B.

Figures 22A, 22B through 31A, 31B illustrate the results of ten groups of related process steps that may be used to produce the apparatus shown in Figure 8. Figures 22A and 22B cross-sectional views defined by the planes indicated as  $X_1^{\prime}X_2^{\prime}$  and  $X_1^{\prime}X_2^{\prime}$ , respectively, in Figure 21; and



SEP/N-799

the other Figures in this group have similar
interpretations.

Figure 32 is a graphic view comparing the p dopant concentration as a function of horizontal distance into the p body portion of the channel region of a transistor cell, before and after formation of the sacrificial oxide layer at the edge of the trench as a result of preferential segregation of p dopant in the sacrificial oxide layer.

Figure 33 is a graphic view of the n+ region, p body region and n- epitaxial layer dopant profiles, before and after formation of the sacrificial oxide layer at the edge of the trench, as a result of preferential segregation of p dopant in the oxide layer and of p dopant in the silicon (p+ and p-).

14 15 16

17

37

38

3

**4** 5

6

7

8

9

10

11

12 13

#### DETAILED DESCRIPTION

### (A) DEVICE DESCRIPTION

18 Figure 1 illustrates a representative MOSFET with the 19 gate positioned in a vertically oriented rectangular trench, 20 as shown in the prior art. This structure is often called a 21 trench vertical DMOSFET. It is "vertical" because the drain 22 contact appears on the back or underside of the substrate 23 and because the channel flow of current from source to drain 24 is approximately vertical. This minimizes the higher 25 resistance associated with bent or curved current paths or 26 with parasitic field effect construction. The device is also doubly diffused (prefix "D") because the source region 27 28 is diffused into the epitaxial material on top of a portion 29 of the earlier-diffused body region of opposite conductivity 30 This structure uses the trench side wall area rather 31 than other silicon surface area for current control by the 32 gate and has a substantially vertical current flow 33 associated with it. This structure is particularly 34 appropriate for power switching transistors where the 35 current carried through a given transverse silicon area is 36 to be maximized.

Two types of trench DMOSFET layouts have been proposed by workers in the field, and these are shown in Figures 2A

SEP/M-799 PATENT

and 2B. The open-cell or stripe geometry shown in Figure 2A
has been reported in papers published by Matsushita Electric
Company in Japan and by General Electric Company in the

4 United States. This implementation results in a surface

5 packing density that is superior to the closed-cell geometry

6 illustrated in Figure 2B. However, the open-cell or stripe

7 geometry is inherently more susceptible to "bipolar

8 breakdown," which is controlled in part by the resistance

between the intrinsic body region below the gate region and

10 the body contact.

9

32

33

34

35 36

11 Figure 3A shows the current versus voltage (I-V) 12 characteristics of an open-cell DMOSFET built by the 13 inventors hereof; this structure has p+ diffused body 14 contacts placed perpendicular to the trench or trenches, and 15 the distance between body contacts is 180 µm, which is relatively large. When the drain voltage exceeds a certain 16 17 breakdown value, the bipolar breakdown phenomenon is 18 manifest where the drain current increases prematurely for 19 drain voltages below the drain-source junction breakdown 20 voltage (BVDSS). Figure 3B shows the output I-V 21 characteristics of a similar transistor with more closely 22 spaced body contacts, about 40 µm; this structure does not display the type of breakdown that is exhibited in Figure 23 24 However, the transistor corresponding to Figure 3B is incapable of carrying as much current as does the device 25 26 that corresponds to Figure 3A, because of the greater body 27 contact area in the Figure 3B structure. An engineering 28 trade-off must be made between on-resistance, breakdown 29 voltage and other engineering figures of merit so that the 30 perimeter-to-area ratio Z/A advantage of the open-cell is 31 lost.

Given these constraints, the closed-cell geometry appears to be more practical. However, the closed-cell geometry has at least three associated problems that do not appear to have been reported on in the technical or patent literature.

The first problem is semiconductor surface breakdown.

The structure shown in Figure 1, whether built in an open-



cell or in a closed-cell geometry, has its body-drain 1 junction terminated perpendicular to the long direction of 2 the trench. This junction is thus exposed to electric field line crowding and to breakdown in the epitaxial material 4 adjacent to the bottom corners of the trench, when the 5 device is biased in the BVDSS condition. This semiconductor 6 surface breakdown carries with it an undesirable hot carrier 7 injection effect, whereby high energy mobile carriers 8 (holes, where the device is an n-channel MOSFET) are 9 transported into the gate oxide. These carriers, created as 10 electron-hole pairs by avalanche multiplication, are 11 accelerated by the presence of the strong electric field, 12 and some of the carriers of a given type (electrons or 13 holes) reach the silicon-oxide interface with sufficient 14 energy to overcome the energy barrier (approximately 3.65 eV 15 for holes) present at the interface and thus move into the 16 oxide. Hot carrier injection will occur if the position of 17 maximum electrical field is within one mean free path (in 18 the silicon) of the silicon-oxide interface. If no special 19 precautions are taken, the maximum electrical field in the 20 21 structure shown in Figure 1 will unavoidably be at the interface so that hot carrier injection will occur as 22 23 illustrated in Figure 4. In a n-channel (p-channel) DMOSFET, hot carrier 24 injection leads to a positive (negative) charging of the 25 gate oxide and the creation of a local electrical field that 26 counteracts the electrical field provided by the gate 27 28 voltage. The result is that the total electrical field in the nearby silicon is relaxed, relative to what the field 29 would be in the absence of hot carrier injection, and the 30 electrical field in the oxide is stressed further. 31 relaxation of electrical field in the silicon causes an 3.2 33 increase in the local breakdown voltage BVDSS. 34 increase in breakdown voltage, commonly called "breakdown 35 walk-out," indicates the presence of otherwise-unobservable hot carrier injections in the gate oxide region. 36 increase in BVDSS is not harmful, but the stressing of the 37 gate oxide is a reliability concern because carrier 38

SFR/M 799 PATENT

injection can ultimately lead to irreversible oxide
breakdown. Experiments have shown that electronic charges,
after injection into silicon, are permanently trapped there
at room temperature.

We have made measurements on test devices and have performed computer simulations that have revealed the presence of unacceptably heavy avalanche injection in trench DMOSFET structures that are made with no special provision to suppress semiconductor surface breakdown. Figure 5 exhibits the results of one computer simulation, where the brackets placed on the electrical field lines indicate the areas of high electrical field strength (greater than 3x105 volts/cm in this example). Surface breakdown occurs adjacent to a trench corner in this example. breakdown can be forced into the bulk of the silicon material, away from the trench and gate oxide, the junction breakdown is no longer associated with irreversible oxide phenomena.

Equally important to the hot-carrier injection problem, surface breakdown is undesirable from the point of view of position of the source of avalanche-generated carriers relative to the body contact. If surface breakdown takes place adjacent to the trench, holes (electrons) flow laterally inside the p- (n-) region, toward the body contact. This forward biases the source-to-body junction and brings the transistor into a bipolar breakdown mode, latch-back. Hence, for a latch-back-free design, the drain breakdown must be controlled such that breakdown occurs on the contact side of the p- (n-) region, thus avoiding lateral current flow in the high-resistivity body region.

Planar DMOS transistors do not have the surface breakdown problem, due to their intrinsic topology. These transistors use the merger at the surface of depletion regions of two adjacent cells, under the gate, thus uniformizing the field structure at the surface. In other words, the planar transistors benefit from the field shaping determined by cell placement.

Figure 6 illustrates merging of the depletion regions

SFP/M 799 PATENT

of two adjacent cells of a planar DMOS transistor, when the gate region 30 and source 28 are set at a common voltage of -500v and the drain region 23 is maintained at 0 volts. The arrows in Figure 6 indicate paths across the depletion region that may produce avalanche breakdown across the p-n junction formed between the body region 27 and the epi layer 25 in a planar DMOS transistor. Typically, breakdown occurs near a curved region of the junction.

A second problem is oxide dielectric breakdown. 9 closed-cell geometry, the trench side wall oxide is grown 10 under nonplanar, two-dimensional conditions at intersections 11 This causes nonplanar, viscous deformation 12 of trench faces. and stress in the adjacent gate oxide material. According 13 14 to published theoretical and experimental evidence, the oxide that grows on the side walls of, for example, a square 15 16 cell DMOS transistor is thinned and distorted at an intersection of two adjacent trench faces in a manner 17 illustrated in Figure 7. When these distortions are 18 19 combined with conformal covering of the surface of gate 20 material, the oxide profile may dev∈lop near-atomically 21 sharp field concentration sites and may manifest premature 22 dielectric breakdown.

23 This problem can be managed and eliminated to some extent by growing and etching away a "sacrificial oxide 24 25 layer" before the gate oxide is grown on the trench walls, 26 as analyzed by Yamabe and Imai, cited above. 27 sacrificial oxidization rounds off the sharp corners of the 28 initial trench profile. This improvement is obtained at the 29 cost of using an additional thermal cycle, during which time 30 an initially shallow impurity profile will diffuse 31 vertically and laterally into the adjacent semiconductor 32 material.

A third problem is the development of clusters of silicon microcolumns known as "black silicon" during the trench etch process. Black silicon occurs as a result of the presence of materials (such as defect clusters) on the silicon surface that have etch rates lower than that of the silicon itself; these materials act as micromasks that SFP/M-799 PATENT

prevent the etching of the silicon microcolumns. materials may result from either an incomplete removal of an oxide trench mask, or they may be deposited on the surface during the trench etch process. The probability of 4 obtaining black silicon has been observed to increase with an increase in the area of exposed silicon and to increase where the silicon area is not closely surrounded by reflecting walls, for example at the intersection of two trench faces. This may result from variations in efficiency 9 of sputter etching of the micromasking materials. 10 Figure 8 illustrates one embodiment of the invention, 11 showing half of a hexagonally shaped trench DMOS structure 12 The structure includes, in this embodiment, an n+ 13 substrate 23, on which is grown a lightly doped epitaxial 14 layer (n) 25 of a predetermined depth depi. Within the epi 15 layer 25, a body region 27 of opposite conductivity (p, p+) 16 is provided. Except in a certain central region that will 17 be discussed shortly, the p body region is substantially 18 planar and lies a distance  $d_{min}$  below the top surface of the epi layer 27. Another covering layer 28 (n+) overlying most 20 of the body region 25 serves as source. A hexagonally 21 shaped trench 29 is provided in the epitaxial layer, opening 22 23 toward the top and having a predetermined depth dtr. trench 29 associated with a transistor cell defines a cell 24 region 31 that is also hexagonally shaped in horizontal 25 cross-section. Within the cell region 31, the body region 26 rises to the top surface of the epi layer 25 and forms an 27 28 exposed pattern 33 in a horizontal cross section at the top 29 surface of the cell region. This central exposed portion of 30 the body region is more heavily doped (p+) than the substantially planar remainder of the body region. Further, 31 32 this central portion of the body region extends to a depth  $d_{\text{max}}$ , below the surface of the epi layer 25, that is greater 33 than the trench depth dtr for the transistor cell. The 34 distance from the deepest part of the (p+) body region to 35 the substrate-epi layer junction is less than the depletion 36 width of a planar p+/n junction that has the same doping 37 profile and is reverse biased around its breakdown 38

SPP/M-799 PATENT

voltage. That is, a central portion 27c of the body region lies below a plane that is defined by the bottom of the 2 trench 29 for the transistor cell. The transistor cell 21 3 4 need not have a hexagonal shape for basic transistor operation; any polygonal shape will suffice, but a regular 5 rectangular shape and a regular hexagonal shape are the most 6 7 convenient for layout purposes as these shapes allow a regular tessellation of the plane. A triangular shape, 9 although it also allows a tessellation of the plane, is not attractive as the sharp trench corners for a triangular-10 11 shaped cell are undesirable.

12 The embodiment of the invention illustrated in Figure 8 13 has several important features: (1) a horizontal section of 14 the transistor cell shows a hexagonally shaped trench, used 15 to suppress oxide dielectric breakdown and for other 16 beneficial purposes; (2) the trench vertical depth is less than the depth of the deepest part of the body region, to 17 18 force voltage breakdown away from the trench surfaces and 19 into the bulk of the semiconductor material; and (3) the 20 intersection of adjacent trench "legs" forms a triangular 21 region with reduced area, for purposes of diminishing the 22 growth of black silicon columns. As noted, a deep body 23 diffusion is included in the center of the transistor cell 24 21 where the body contact is to be made. This diffusion is 25 deeper than the trench depth by an amount that depends upon gate oxide thickness and upon epitaxial silicon resistivity 26 27 so that the semiconductor breakdown is forced away from any 28 trench surface or corner and into the bulk of the 29 semiconductor material, namely inside the field-constricted 30 region created by the deep body junction and the adjacent 31 substrate ("reach-through bulk breakdown"). Using this 32 diffusion profile, the breakdown voltage of the transistor 33 is relatively stable and hot carrier injection is 34 suppressed. Moreover, avalanche breakdown occurs below the 35 body contact, not laterally along the contact, and lateral 36 voltage drop through the body region, which would lead to 37 bipolar breakdown, is avoided. The reverse breakdown I-V 38 characteristic of the transistor cell has an abrupt or

SEP/M 199 PATENT

"hard" appearance because it is determined by bulk
breakdown, and it takes place relatively uniformly in the
active area. The transistor cell is free of high current
concentration (avalanche) and is free of bipolar breakdown
and can thus carry reverse avalanche currents that are
comparable in magnitude to the forward current; this may be
useful in some applications.

8

9

10

11

12

13

14

15 16 Figure 9 shows the results of a computer simulation of BVDSS operation of a trenched DMOS transistor constructed according to the invention, where the deepest part of the deep body region lies below the bottom of the trench. The field structure illustrated in Figure 9 reveals bulk semiconductor breakdown, as desired. This should be compared to the structure illustrated in Figure 5 in which the deepest part of the body region lies above the bottom of the trench and in which surface breakdown prevails.

17 In a horizontal cross-section, the trench side walls 18 intersect at angles of approximately 120°, as compared to an 19 intersection angle of 90° in a rectangular cell design. 20 This offers a substantial improvement for two-dimensional 21 oxidation conditions as it reduces stress at the corners and 22 promotes increased uniformity of oxide thickness. Further, 23 the hexagon corners may become rounded off during the trench 24 mask lithography and etching processes that precede trench 25 formation so that the DMOS cells approach the cylindrical 26 shape of a natural, field-controlled current valve. 27 hexagonal cell, trench DMOS is expected to have a higher 28 gate rupture breakdown voltage than does its rectangular 29 cell counterpart. For transistor operation the trench 30 shape, in horizontal cross section (plan view), may be a 31 polygon (not necessarily regular) or a circle or an oval; 32 but the regular hexagon and polygonal shapes approaching a 33 circle are the preferred shapes from the point of view of 34 maximizing the gate oxide rupture voltage.

With reference to Figure 10A, the open area at the trench intersection for a rectangular design is b<sup>2</sup>, where b is the trench width. By contrast, for the hexagonally shaped trench design (Figure 10B), the open area at a trench

cells is

intersection is  $\sqrt{3}b^2/4 = 0.43b^2$ , a reduction by more than 1 2 50% in the corresponding open area relative to the conventional rectangular design. As noted earlier, the 3 probability of formation of black silicon columns increases as the open area at trench intersections increases, so that 5 a hexagonally-shaped trench will be less susceptible to the 6 7 black silicon problem than its rectangular cell counterpart. Further, one can show that the hexagonal 8 shaped cell design has the same Z/A figure of merit as does 9 a square cell design with the same cell opening, a, and the 10 same trench width, b. The Z/A parameter for each of these 11

12

15

16 17

.13

 $\frac{Z}{A} = \frac{4a}{(a+b)^{2}}$ Thus, the linear region of resistance of a hexagonal cell, 14 trench DMOS transistor is neither superior to nor inferior to the corresponding square cell transistor that occupies the same silicon area.

18 Figure 11 illustrates graphically the approximate 19 doping concentration taken along a cross-section line CC 20 that is adjacent to a trench 29, as indicated in Figure 8. 21 Distance, shown in microns along the abscissa of Figure 11, is measured from the top surface of the cell. Beginning at 22 23 the top surface and moving down, the first layer is an n+ source region 28 with a maximum n type doping concentration (at the surface) of approximately  $10^{20}$  cm<sup>-3</sup>; this extends to 25 a depth of approximately 1 µm. The next dopant layer 26 27 encountered is a p type body region 27, having a maximum concentration of approximately 7 x  $10^{16}$  and decreasing as 28 29 the distance from the top surface increases; the body region 30 27 extends from a first junction (source-body) at 31 approximately 1 µm depth to a second junction (body-epi 32 layer) at approximately 2.7 µm depth. The next layer 33 encountered is an n type epitaxial layer 25 having an approximately constant doping concentration of about 5 x 34  $10^{15}$  cm<sup>-3</sup> and extending from the second junction point at 35 36  $2.7 \mu m$  depth to a transition region that is located at a 37 depth of 6 µm. An n+ drain region 23 lies below and is 38 contiguous to the epitaxial layer 25; doping concentration

SEP/M-799 PATENT

1 in the n+ drain region 23 increases from about  $5 \times 10^{15}$  cm<sup>-3</sup> 2 to a maximum value of approximately  $5 \times 10^{18}$  cm<sup>-3</sup> as the 3 depth increases.

Figure 12 exhibits the doping concentration along a 4 deep body line DD shown in Pigure 8. At the top surface, a heavily-doped p type body region 28 of maximum concentration 6 approximately 7 x  $10^{19}$  cm<sup>-3</sup> (at the top surface) is present 7 and extends from the top surface to a depth of approximately 4.5 $\mu m$ . An n type epitaxial layer of doping concentration substantially 5 x  $10^{15}$  cm<sup>-3</sup> extends from a first junction at 10 4.5µm to a transition region at approximately 6µm. 11 depth of  $6\mu m$ , the heavily doped n+ drain, having maximum 12 concentration of substantially 5 x  $10^{18}$  cm<sup>-3</sup> is positioned 13 contiquous to the n type epitaxial layer. All dopant 14 15 profile data in Figures 11 and 12 here refer to a low voltage (~60 volts breakdown) trench DMOS transistor. 16

The absolute depth of the p+ deep body region 27C 17 (shown as approximately 4.5  $\mu m$  in Figure 12) is not of 18 controlling importance for the position of initial breakdown 19 in the transistor cell. The important parameters are 20 (1) the difference between the p+ region depth (called 21 22 simply "junction depth" here) and the trench depth, (2) the difference between the depth of the bottom surface of the 23 24 epitaxial layer 25 and the bottom of the p+ deep body region 25 27c (shown as approximately 1.5µm in Figure 12) and (3) the 26 gate oxide thickness.

27

28

29

30

31

32

33 34 We have performed extensive simulations to identify the initial point of voltage breakdown in a transistor cell of the configuration illustrated in Figure 8, using the PISCES program available from Technology Modeling Associates, Palo Alto, California. Avalanche breakdown occurs by definition at the point, if any, along an electric line  $(x_0 \le x' \le x)$  for which the current multiplication integral equals one; that is

35
36 
$$\int_{\alpha}^{x} \alpha_{n}(x') \exp\left[\int_{x_{0}}^{x'} (\alpha_{p}(x'') - \alpha_{n}(x'')) dx''\right] dx' = 1, \quad (1)$$
37

38 where  $\alpha_n(x)$  and  $\alpha_p(x)$  are carrier ionization coefficients



38

for electrons and holes, respectively, that depend upon the local electrical field strength E and other variables. Two positions of interest for initiation of avalanche breakdown are (1) a point P<sub>1</sub> in the channel region adjacent to a corner of the trench and (2) a point P<sub>2</sub> in the bulk of the semiconductor material that is spaced apart by several microns from the trench and channel region. Avalanche breakdown adjacent to the trench is undesirable; avalanche breakdown, if it occurs at all, in the bulk of the material at a position such as P<sub>2</sub> is acceptable, for the reasons discussed above.

12 In our simulations, the n+ source region 28 and the 13 gate region 29 were both held at 0 volts, according to the 14 customary definition of drain breakdown voltage BVDSS. voltage of the drain region 23 was increased incrementally, 15 16 beginning at 0 volts (without ionization integral 17 calculation) and from 50 volts upward in one-volt increments 18 (with calculation of the ionization integral value from 19 Eq. (1)), until the avalanche breakdown equation shown above 20 was satisfied at some point along a current flow line. 21 point for which avalanche breakdown first occurs (i.e., with 22 the lowest drain voltage) is identified as the point of 23 initial avalanche breakdown.

24 We found, surprisingly, that if initial avalanche 25 breakdown is to occur in the bulk rather than adjacent to a 26 trench corner, it is not sufficient that the junction depth 27 be at least equal to the trench depth; junction depth minus trench depth must exceed a lower bound that is approximately 28 29 0.5µm and may be greater in some situations. This is 30 illustrated in Figures 13, 14 and 15. In Figure 13, the 31 trench depth and the junction depth are approximately equal, 32 each being about 3.5  $\mu m$  below the top surface of the 33 transistor cell; epitaxial layer thickness, measured from 34 the top surface, is  $5.25 \mu m$ . In this situation, avalanche 35 breakdown is initiated adjacent to a corner of the trench 36 indicated by an X, when the drain voltage reaches 37 approximately 64.2 volts.

In Figure 14, trench depth is 3.5 µm and junction depth

SPT/M-799

- 1 is 4  $\mu$ m; epitaxial layer thickness is 5.25  $\mu$ m. Avalanche
- 2 breakdown is initiated adjacent to a corner of the trench
- 3 when the drain voltage reaches approximately 65.2 volts. A
- 4 slight improvement is breakdown voltage occurs, but
- 5 avalanche breakdown is still initiated adjacent to a corner
- 6 of the trench, which is undesirable.
- 7 In Figure 15, the trench depth is 3.5 µm but the
- 8 junction depth is about 4.5 μm; epitaxial layer thickness is
- 9 5.25 µm. Here, avalanche breakdown is initiated in the bulk
- 10 of the material, at the position marked X, and the
- 11 associated breakdown voltage is approximately 61.8 volts.
- 12 In Figures 13, 14 and 15, the gate oxide thickness was 0.1
- 13 µm.
- Another variable of importance here is the difference
- 15 between junction depth and depth of the bottom surface of
- 16 the epitaxial layer. Avalanche breakdown at a point in the
- 17 bulk at the junction is of the nature of a reach-through
- 18 breakdown across the epitaxial layer. Thus, the epitaxial
- 19 layer should not be too great or reach-through breakdown
- 20 across the epitaxial layer may not occur; and initiation of
- 21 avalanche breakdown in the bulk may become impossible or
- 22 very difficult, even where the junction depth is much larger
- 23 than the trench depth.
- In Figures 16 and 17, the gate oxide thickness is
- 25 0.10  $\mu m$  and the epitaxial layer thickness in the region of
- 26 maximum junction depth is decreased from 5.25 µm in Figure
- 27 14 to 5  $\mu$ m (Figure 16) and to 4.5  $\mu$ m (Figure 17). Where the
- 28 junction depth is only 0.50µm larger than the trench depth,
- 29 avalanche breakdown is initiated adjacent to a trench corner
- 30 for epi layer thickness that is decreased to 5.0  $\mu m$
- 31 (Figure 16) and to 4.5 µm (Figure 17). The corresponding
- 32 drain-source breakdown voltages are 61.25 volts (Figure 16)
- 33 and 52.7 volts (Figure 17). As would be expected, drain-
- 34 source breakdown voltage decreases markedly as the epi layer
- 35 thickness is decreased.
- 36 A third variable of importance here is the thickness of
- 37 the oxide layer separating the gate material 29 (for
- 38 example, doped polysilicon) from the surrounding n-type and

SEP/H 799

1 p-type semiconductor materials. If the gate oxide thickness is increased, the gate oxide can take up a larger portion of 3 the stress associated with the local electrical field, and 4 initiation of avalanche breakdown adjacent to the trench 5 becomes less likely. However, if the gate oxide thickness is increased, the on-state resistance is also increased 7 (undesirable) and the gate voltage has less effect on current flow in the channel region; for this reason, the 9 gate oxide thickness probably should not be increased beyond 10 0.20 µm. The field-shaping that can be accomplished by increasing the oxide thickness becomes more efficient as the 11 12 breakdown voltage specified for the transistor increases; in higher-voltage transistors, the channel resistance makes a 13 14 proportionately smaller contribution to total on-resistance. 15 Figures 18 and 19 illustrate the effect of increasing 16 the gate oxide thickness  $t_{ox}$ , originally set at 0.10  $\mu m$ , on 17 the initiation of avalanche breakdown. In each of Figures 18 18 and 19, the trench depth is 3.5µm and the junction depth is 4  $\mu$ m. As noted above in the discussion of Figure 14, 19 20 with  $t_{OX} = 0.1 \mu m$ , avalanche breakdown is initiated adjacent to a corner of the trench, when the drain source voltage 21 reaches 65.2 volts. When the gate oxide thickness is 22 23 increased to  $t_{Ox}$  = 0.14  $\mu m$  (Figure 18), avalanche breakdown 24 is still initiated adjacent to the trench corner and the 25 drain-source voltage at breakdown is 67.5 volts. With the oxide thickness increased to  $t_{Ox} = 0.20 \mu m$  (Figure 19), 26 27 avalanche breakdown is initiated in the bulk, adjacent to a 28 point on the deep body-epitaxial layer junction that is 29 spaced apart from the trench, and the drain-source voltage at breakdown is increased to 69.6 volts. Where a gate oxide 30 31 thickness of  $t_{ov} = 0.20 \mu m$  is used, the on-state resistance 32 of the channel region is increased to possibly-unacceptable 33 values in low-voltage transistors. However, gate oxide 34 thickness is a control variable for positioning of the 35 initial point of avalanche breakdown and for control of the 36 associated breakdown voltage: Ceteris paribus, as tox 37 increases, the drain-source breakdown voltage increases and 38 the point of initial avalanche breakdown tends to move away

SFF/M-799 PATENT

1 from the trench and into the bulk material, as desired.

- Figure 20 illustrates the point of initiation of avalanche
- B breakdown for trench depth = junction depth = 3.5 μm and
- 4  $t_{OX} = 0.20 \mu m$ : The point of initiation of avalanche
- 5 breakdown remains adjacent to a trench corner, even for a
- 6 relatively large gate oxide thickness.
- 7 Figures 13-20 illustrate the control of the point of
- 8 initiation of avalanche breakdown based upon parameters such
- 9 as (1) the difference between (maximum) junction depth and
- 10 trench depth, (2) thickness at the deepest part of the
- 11 junction of the epitaxial layer and (3) gate oxide
- 12 thickness. The numbers used in Figures 13-20 are represen-
- 13 tative of the situations discussed in connection with these
- 14 figures. The values of the parameters themselves will vary
- 15 with the magnitude of doping concentrations in the
- 16 semiconductor materials as well as with other semiconductor
- 17 parameters. The field shaping technique described herein is
- 18 also applicable to open-cell or stripe geometry transistors
- 19 that have deep body regions positioned between adjacent
- 20 trenches.

21 22

## (B) PROCESS DESCRIPTION

- Figures 22A and 22B are schematic cross-sectional views
- 24 of a transistor cell shown in plan view in Figure 21, where
- 25 the cross-sectional views are taken with respect to planes
- 26 indicated by the lines  $X_1X_2$  (Figure 22A) and  $X_1X_2$
- 27 (Figure 22B) for a first related group of process steps. In
- 28 this first group of process steps, the operator (la)
- 29 provides a heavily doped (n+) substrate 23 of resistivity
- 30 substantially 0.005-0.01 Ohm-cm and thickness substantially
- 31 500  $\mu$ m; (1b) provides a covering layer 25 of the same
- 32 conductivity type as the substrate but of lower doping
- 33 (resistivity substantially 1 Ohm-cm) and of thickness
- 34 substantially 6-7  $\mu$ m; (1c) provides an oxide of thickness
- 35 substantially 0.6 µm on the surface of layer 25;
- 36 (ld) provides a first mask over the oxidized surface of the
- 37 covering layer 25 with a first aperture therein of diameter
- 38 substantially 3-4 µm, and etches away the oxide exposed

SPD/M-799

38

1 within the aperture; (le) provides a thin implant oxide (not shown) of thickness substantially 450 Å on the upper silicon surface exposed by step 1d; (1f) uses ion implantation of second conductivity type (for example, B ions that correspond to dopant of p type) of energy substantially 60 5 keV and dose substantially 3.2 x  $10^{15}$  cm<sup>-2</sup> to convert an upper portion 27a of the covering layer 25 from n type 7 8 (first conductivity type) to p+ type (second conductivity type) of thickness substantially 450 Å, as indicated in 10 Figures 22A and 22B; (1g) provides an anneal and drive-in in the presence of N2 gas for a time interval of substantially 11 12 10 minutes at a temperature of substantially T = 1050°C; and 13 (lh) provides a drive-in in the presence of wet 0, for a time interval  $\Delta t = 60$  min. at a temperature of T = 950°C, 14 15 leaving an oxide thickness (2600 Å) on the top surface of 16 the structure including the p+ region. 17 In a second group of related process steps, indicated 18 in Figures 23A and 23B, the operator (2a) provides a mask 19 over the upper surface of the structure with a second 20 aperture therein of predetermined size and position adjacent 21 to and partly overlapping the first aperture (step lc), and 22 etches away the oxide [produced in the drive-in operation of 23 steps (lg) and (lh)] that is exposed within the second 24 aperture; (2b) provides a thin implant oxide (not shown) of 25 thickness substantially 450 Å on the upper silicon surface 26 exposed by step (2a); (2c) provides ion implantation of ions 27 of second conductivity type (for example, B ions) of energy substantially 60 keV and dose substantially 2.7  $\times$  10<sup>13</sup> cm<sup>-2</sup> 28 29 to convert a second upper portion of the covering layer 25 30 from n type to p type, where the first ion implant region 31 27a (p+) and the second ion implant region 27b (p) may have 32 an overlap region 27c in a lateral direction to provide a transition region from p to p+ as indicated in Figures 23A 33 34 and 23B; (2d) provides a drive-in of the ions in regions 35 27a, 27b and 27c for a time interval of substantially 36 120 min. at a temperature of substantially T = 1150°C, and 37 removes any oxide grown in regions 27b and 27c during this



drive-in; (2e) provides a thin implant oxide layer of

SFE/M 799 PATENT

1 thickness substantially 300 % on the upper silicon surface 2 of regions 27b and 27c; (2f) provides a mask with a 3 third aperture therein, the aperture exposing substantially 4 all of the p region 27b and of the p/p+ transition region 27c; (2g) provides an ion implant of second conductivity 6 type (for example, As) of energy substantially 80 keV and 7 dose substantially 5.8 x  $10^{15}$  cm<sup>-2</sup> to convert an upper portion 28 (of thickness substantially 1600 Å) of the p region 27b and the p/p+ region 27c from second conductivity 10 type (p) to heavily doped first conductivity type (n+), as 11 illustrated in Figures 23A and 23B; and (2h) deposits low 12 temperature oxide 34 as a mask over the upper surface of the 13 structure, for later use as a trench mask.

14 Figures 24A and 24B indicate the results of a third 15 related group of process steps. In this third group of 16 process steps, the operator (3a) provides a photoresist mask 17 for selective etching of the low temperature oxide layer 34; 18 (3b) removes the photoresist; (3c) uses a high anisotropy 19 etch to produce a trench 29 that is substantially 20 rectangula: or trapezoidal in a vertical cross-section 21 (Figure 24A); the trench 29 has a predetermined depth 22 relative to the top surface of the structure of 23 substantially  $d_{tr}$  = 3-4  $\mu m$ ; and (3d) removes the remaining 24 low temperature oxide layer and the source implant oxide 25 layer to expose the n+ area 28.

26 Figures 25A and 25B show the results of a fourth 27 related group of process steps, wherein the operator (4a) 28 grows a sacrificial oxide layer (not shown) of thickness 29 substantially 3500 Å, using a steam environment at a 30 temperature of substantially T = 1100°C for a time interval 31 of substantially  $\Delta t = 20 \text{ min.}$ , over the upper surface of the structure including the exposed bottom and side walls of the 33 trench 29; (4b) removes all of the sacrificial oxide layer, 34 using a wet etch, leaving the rounded corners of the trench 35 29 produced by the sacrificial oxide growth; and (4c) grows a gate oxide layer 35 of thickness substantially 1200  $\mbox{\normalfont\AA}$ , using a dry O2 environment at a temperature of substantially 1050°C for a time interval of substantially At = 90 min.



SFP/M-799 PATENT

1 Figures 26A and 26B show the results of a fifth related 2 group of process steps, wherein the operator (5a) deposits a 3 first polysilicon layer 36 (post-doped or doped in situ) of 4 thickness substantially 7500 Å on the gate oxide layer 35, 5 including the gate oxide on the bottom and side walls of the 6 trench 29; and (5b) grows an oxide layer 37 (etch-stop 7 oxide) of thickness substantially 1500 Å on the first 8 polysilicon layer 36.

Figures 27A and 27B show the results of a sixth process step, wherein the operator (6a) deposits a second polysilicon layer 38 (undoped) of thickness substantially 3  $\mu$ m over the oxide layer 37 and in the trench 29 to fill any portion of the trench that is not yet filled.

9

10

11

12

13

14 Figures 28A and 28B show the results of a seventh 15 related group of process steps, wherein the operator (7a) 16 removes substantially all of the second polysilicon layer 38 17 at the upper surface of the structure, not including the 18 polysilicon deposited in the trench 29; this removes most or 19 all of the cusp 39c that is otherwise manifest at the mouth 20 of the trench 29 so that the upper surface of the structure 21 is substantially planar; the etch-stop oxide layer 37 is 22 used for monitoring purposes, to determine when to stop the 23 etching process for the second polysilicon layer so that the process does not remove the remainder of the second polysilicon layer 38 from the trench; and (7b) removes the 25 26 etch-stop oxide layer 37 from the upper surface of the 27 structure, not including the portion of the etch-stop oxide 28 layer that is located in the trench 29.

29 Figures 29A and 29B show the results of an eighth 30 process step, wherein the operator (8a) masks and etches a 31 portion of the exposed first polysilicon layer 36 that is 32 adjacent to but not within the trench 29, for the 33 cross-sectional view illustrated in Figure 29A. As a result 34 of this step, any electrical connection between the portion 35 36a of the first polysilicon layer that lies within the 36 trench 29 and the portion 36b of the first polysilicon layer 37 that lies outside the trench is severed in the area shown in 38 this cross-section. The portion 36a of the first



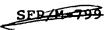
1 polysilicon layer that lies within the trench will be used 2 for gate voltage control; electrical contact to this 3 polysilicon layer is made through the continuous (unsevered) 4 polysilicon shown in cross-section in Figure 29B. 5 Figures 30A and 30B show the results of a ninth related group of process steps, wherein the operator (9a) grows a 6 7 thin layer of oxide over the upper surface of the structure, 8 including the two segments 36a and 36b of the first 9 polysilicon layer; (9b) deposits a BPSG layer 41 of thickness substantially 0.8 µm at a temperature of 11 substantially T = 400°C over the upper surface of the structure; (9c) applies a contact mask at selected positions 12 13 on the BPSG layer 41 and etches apertures in the BPSG to 14 open electrical contact areas for the source region 28, the 15 heavily doped portion 27 of the body region and the gate 16 (doped polysilicon) region 36b; and (9d) raises the 17 temperature of the BPSG layer 41 to substantially T = 900°C 18 for a time interval of substantially  $\Delta t = 30$  min. and allows 19 reflow of the BPSG material to fill in and round off the 20 sharp exposed areas produced by the contact area etch. 21 Figures 31A and 31B show the results of a tenth related 22 group of process steps, wherein the operator (10a) deposits 23 a metallization layer (for example, Al/Si) over the upper surface of the structure; (10b) masks and etches the 25 metallization layer into separate regions 43a (gate) and 43b 26 (source/body) to separate the gate and source/body contacts; 27 (10c) alloys the metallization material with the silicon 28 surface in regions 27 and 28, and with the doped polysilicon 29 region 36b; (10d) deposits a passivation layer (not shown, 30 optional) such as Si<sub>3</sub>N<sub>A</sub>H<sub>Y</sub> by a PECVD process over the upper 31 surface of the structure and etches apertures in the 32 passivation layer to open electrical contact areas to the 33 gate and source/body regions; and (10e) installs a drain 34 contact 45 at the bottom surface of the substrate 23. 35 result of these process steps in one embodiment is the 36 hexagonally-shaped transistor cell shown in a three-37 dimensional representation in Figure 8. 38 Figure 21 and Figures 22A/22B through 31A/31B

1 illustrate the configuration and the process steps for the 2 active region (where the transistor cells are located and 3 where electrical contact is made to the source and body of 4 the transistor), and for the field region that lies adjacent 5 to the active region (where electrical contact is made to 6 the gate).

The metallization layer 43b shown in Figure 31A is used 7 to control the voltage of the source region 28, and to 8 assure electrical contact between the source region 28 and 9 the p+ region 27, to maintain the source and body of the 10 transistor at the same potential. This metallization layer 11 is confined within the active region and is electrically 12 isolated from the gate (doped polysilicon in the trench) by 13 the BPSG layer 41, as shown in Figure 31b. 14

Because the source/body metallization layer 43b covers 15 substantially all of the active region, the electrical 16 contact to the gate must be made in the field region. 17 order to accomplish this, the trench 29 (containing the 18 doped polysilicon) extends beyond the boundary of the active 20 region to a portion of the field region 47 as shown in Figure 21 and Figures 24A/24B. Figure 29A indicates that, 21 in the plane  $X_1^{\prime}X_2^{\prime}$ , a cut is made in the doped polysilicon 22 layer on the top surface of the transistor cell so that the 23 doped polysilicon is separated into a first portion 36a that 24 is positioned within the trench 29 and a second portion 36b 25 to which a metallization contact 43a is made as shown in Figure 21 and Figure 31A. However, Figure 29B shows that in 27 the plane  $X^{\bullet}_{1}X^{\bullet}_{2}$ , the doped polysilicon remains uncut 28 (continuous); it extends beyond the end of the trench 29 protruding into the field region, and up onto the surface of 30 the structure, where it makes electrical contact to the gate 31 metallization layer 43a (Figure 21 and Figure 29B). The use 32 of a gate contact that is positioned in a field area outside the active area of the array of transistor cells, ensures 34 the continuity of gate electrode from its metallization 35 contact through a layer of doped polysilicon to the oxidized 36 trench sidewalls in the DMOS transistor cells. This gate 37 contact approach is both topologically and technologically

38



1 different from gate contact approaches used in planar DMOS
2 transistors.

3 Growth of a sacrificial oxide layer at the edge of the 4 trench 29, as discussed in connection with Figures 25A and 5 25B, has two other surprising and beneficial effects in 6 configurations such as those shown in Figure 8. Where a 7 silicon dioxide layer is grown from a silicon layer that is 8 possibly doped with p type dopant and/or n type dopant, the 9 p type dopant will preferentially segregate in the silicon 10 oxide and n type dopant will preferentially segregate in the 11 silicon. Figure 32 graphically illustrates p type dopant 12 concentration in the body zone as a function of distance x 13 from the edge of the trench oxide layer, before growth of 14 the sacrificial oxide layer and after growth of this 15 layer. As a result of growth of this oxide layer contiguous 16 to the p body zone 27, the p type dopant concentration 17 decreases in the channel region adjacent to the oxide-18 silicon interface, as shown in Figure 32. This allows the 19 use of a higher p type dopant concentration in the p body 20 zone 27, so that for a given value of threshold voltage in 21 the channel region, the resistance between the channel and 22 the body contact (p+ region 33) is reduced and bipolar 23 breakdown (latchback) is suppressed.

24 Figure 33 graphically illustrates the junctions or 25 boundaries between portions of the n+ source region 28, the 26 p body region 27 and the n- epitaxial region 25 that are 27 adjacent to the interfaces of these regions with the trench 28 29 (or trench oxide layer), before and after growth of the 29 sacrificial trench oxide layer. As a result of the growth 30 of this oxide layer, the p type dopant concentration is 31 reduced in the region 27 and the n type dopant concentration 32 is increased in the regions 28 and 25. This results in a 33 shortened channel length in the p body zone 27 from source 34 region 28 to epitaxial region 25, which produces superior 35 on-state resistance (i.e., a lower resistance value). 36 conventional method of producing short channel lengths in 37 planar DMOS transistors begins with very shallow junctions; 38 this approach severely limits the number of high temperature

SEP/M-799 PATENT

1 cycles that may be used in formation of the device. 2 technique for achieving short channel lengths disclosed 3 herein, the natural segregation of p type and n type dopants at an oxide-silicon interface is used to shorten the channel length; this approach does not appear to limit the number of 5 6 high temperature cycles used in the formation of the device.

The preferred embodiment discussed here has used an n+ 8 source region 28, p/p+ body region 27, n epitaxial layer 25 and n+ drain region 23. The electrical conductivity types of each of these regions can be simultaneously exchanged (n type + p type, and p type + n type) with no qualitative change in the results.

13 For an n type substrate 23 (Figure 8), substrate 14 resistivity should be of the order of five milliohm-cm so 15 that substrate doping concentration should be at least  $10^{19} \text{cm}^{-3}$ ; for a p type substrate the doping concentration 16 17 should be somewhat higher. For an n type (p type) epitaxial 18 layer 25, the resistivity should be about one Ohm-cm so that 19 the doping concentration should be in the range  $10^{15}-10^{16}$  cm<sup>-3</sup> ( $10^{16}-10^{17}$  cm<sup>-3</sup>). The heavily doped portion 20 21 27c of the body region 27 should be doped to at least  $10^{18} \text{cm}^{-3}$  (surface dopant concentration), and preferably should have a surface dopant concentration of 5x10<sup>18</sup>cm<sup>-3</sup> or 23 24 greater. The lighter-doped portion of the body region 27 may be doped in the range  $10^{16}-10^{17}$ cm<sup>-3</sup>; the details of the 25 26 body profile are not critical, but they must be consistent 27 with a  $5 \times 10^{16} \text{cm}^{-3}$  peak body concentration for threshold 28 voltage to be in the range of 2-3 V. The source region 28 29 must provide a good ohmic contact and should have a surface dopant concentration of at least  $5 \times 10^{19} \text{cm}^{-3}$ . 30

Although the preferred embodiments of the invention 32 have been shown and described herein, variation and 33 modification may be made without departing from the scope of the invention.

35 36

34

31

7

9

10 11

12

37

38